CGMS-XXXI EUM-WP-16
Prepared by EUMETSAT
Agenda Item: II/2

OPERATIONAL CALIBRATION OF THE MSG/SEVIRI SOLAR CHANNELS

An operational algorithm has been developed for the routine calibration of the solar channels of SEVIRI onboard the MSG spacecraft. The calibration method relies on calculated radiances over clear ocean and bright desert sites. The accuracy of these simulated radiances, about 3%, has been established against well calibrated spaceborne observations acquired over the calibration targets. First SEVIRI images have already been calibrated with this method. This paper has been written in response to CGMS action 30.19.

1 INTRODUCTION

As no on-board calibration device is available for the solar channels of MSG/SEVIRI, their calibration has to rely on vicarious methods. This method relies on radiative transfer modelling over bright desert and clear ocean sites. The choice of this method has been driven by the need to fulfil the accuracy and precision requirements of the MSG operational ground segment during the entire duration of the mission, *i.e.*, more than 12 years. Radiative transfer simulations are performed with the 6S code (Vermote et al. 1997) using a data set of surface and atmospheric properties. This data set is used to simulate SEVIRI observations accounting for the exact viewing and illumination conditions as well as the spectral characteristics of the instrument. The duration of the MSG mission prohibits the continuous characterization of a limited number of targets with ground observations. The proposed strategy relies therefore on the definition of a large number of stable targets for which surface properties are estimated once and for all.

The accuracy and precision of these calculated radiances are estimated comparing simulations with calibrated observations acquired by spaceborne instruments such as the Along-Track Scanning Radiometer (ATSR-2) instrument of the European Space Agency (ESA) flying on the European Remote Sensing Satellite-2 (ERS-2), the Sea-viewing Wide Field-of-view Sensor (SeaWiFS) instrument on board the National Aeronautics and Space Administration (NASA) SeaStar spacecraft, the VEGETATION instrument on the french "Système pour l'Observation de la Terre" (SPOT-4) platform and finally the MEdium Resolution Imaging Spectrometer (MERIS) flying on the ESA ENVIronmental Research SATellite (ENVISAT). An operational algorithm, named SEVIRI Solar Channel Calibration (SSCC), has been developed to ensure a routine calibration of the solar channels. First results show that SEVIRI solar channels can be calibrated with an estimated accuracy ranging from 4 to 6%, at the 95% confidence level, according to the band. Verification of these estimations are still on-going.

Table 1: SEVIRI Solar Channel Characteristics. The dynamic range is given in $\mathrm{Wm^{-2}sr^{-1}}\mu\mathrm{m}^{-1}$. The Signal to Noise Ratio (SNR) is given at 1% of the maximum dynamic range. The standard deviation (std. d.) of the Normalized Spectral Response (NSR) characterization error is given in percent. The calibration requirement is given in $\mathrm{Wm^{-2}sr^{-1}}\mu\mathrm{m}^{-1}$.

Channel	Spectral Band (μm)	Dynamic Range	Short-term Noise Perf.	NSR std. d.	Cal. Requ.
HRV	0.37 – 1.25	0 – 460	SNR> 4.6	1.8%	9.18
VIS0.6	0.56 – 0.71	0 – 533	SNR>14.3	1.0%	10.66
VIS0.8	0.74 – 0.88	0 – 357	SNR> 9.7	1.0%	7.14
NIR1.6	1.50 – 1.78	0 – 75	SNR> 3.0	0.8%	1.50

2 THE SEVIRI RADIOMETER

SEVIRI is the main radiometer on board the MSG spacecraft. It scans the Earth disc every 15 minutes within 11 spectral channels located between 0.6μm and 14μm and a high resolution broadband visible channel (HRV). The East-West and South-North sampling distance at the sub-satellite point is 3×3 km (1×1 km for HRV), and the instantaneous field of view is about 5km (2km for HRV). The characteristics of the channels located in the solar spectral region are given in Table (1), where the actual pre-launch radiometric performances are given for the SEVIRI instrument onboard MSG-1. Each spectral channel is composed of three detectors, except HRV with nine. The output signal of all channels is coded on 10 bits. The medium-term (long-term) drift is expected

to be better or equal to 0.1% (2%) of the maximum dynamic range. The normalized spectral response $\xi(\lambda)$ of the solar channels is characterized with a mean relative error of about 1%, which represents a significant improvement with respect to the VIS band of the Meteosat first generation radiometer. The sensor spectral responses (SSR) and associated error are shown on Fig. (1). The SSR total error accounts for errors due to the absolute wavelength calibration uncertainty, the measurement noise and bias of the optic and detector transmittance.

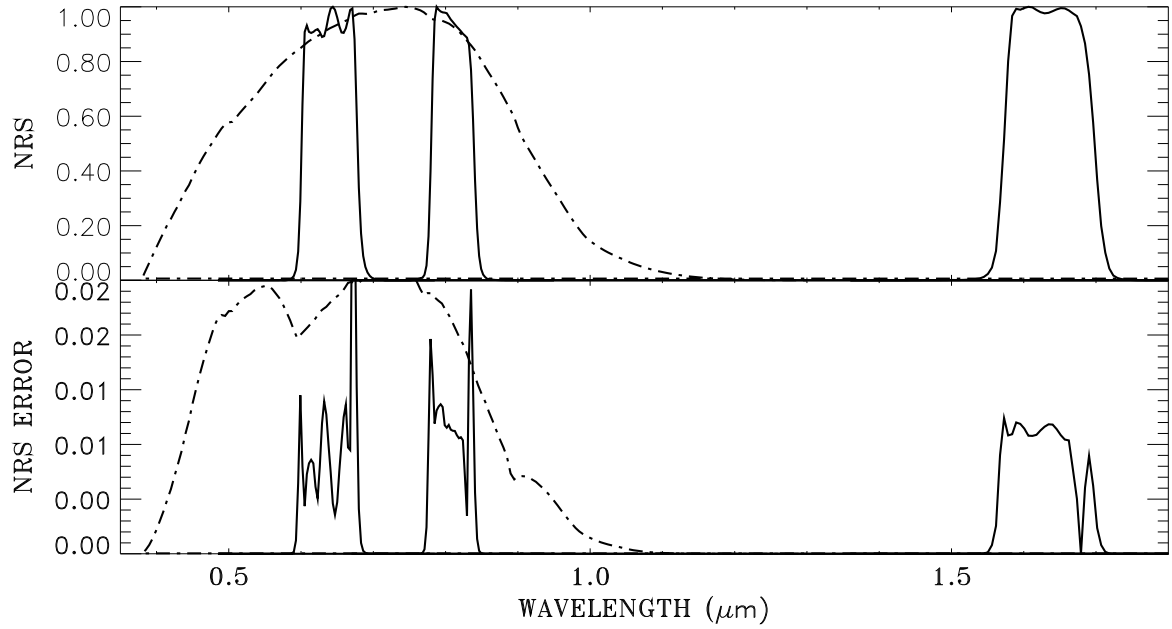

Figure 1: Top: Normalized Spectral Response (NSR) of the SEVIRI solar channels. The response of the HRV band is shown with a dash-dotted line. Bottom: NSR characterization absolute error.

The radiometric preprocessing of level 1.0 data, *i.e.*, the transformation of raw data to level 1.5 geo-located radiances, includes the linearization of the signal, the equalization of the detector output of a same channel and finally the pixel geo-location to a reference grid centered at 0 degree longitude (Schmetz et al. 2002). The image size is 3712×3712 pixels except for the HRV band which has a size of 11136×5568 (SN×EW). The geo-location absolute accuracy is expected to be about one pixel with a root mean square error from image to image less than 0.5 pixel. Ground control points are used to monitor the quality of the geo-location process.

3 CALIBRATION TARGET CHARACTERIZATION

3.1 Overview

The bulk effort concerning the target description essentially consists in the characterization of the calibration target radiative state variables. It is therefore necessary to identify a set of targets for which it is possible to characterize as accurately as possible the atmospheric and surface parameters during a period similar to the MSG mission duration. In order to minimize the characterization effort of the surface properties, the MSG mission lasts more than 12 years, it is preferable to select stable and uniform targets, as can be found in arid desert areas or in open oceans.

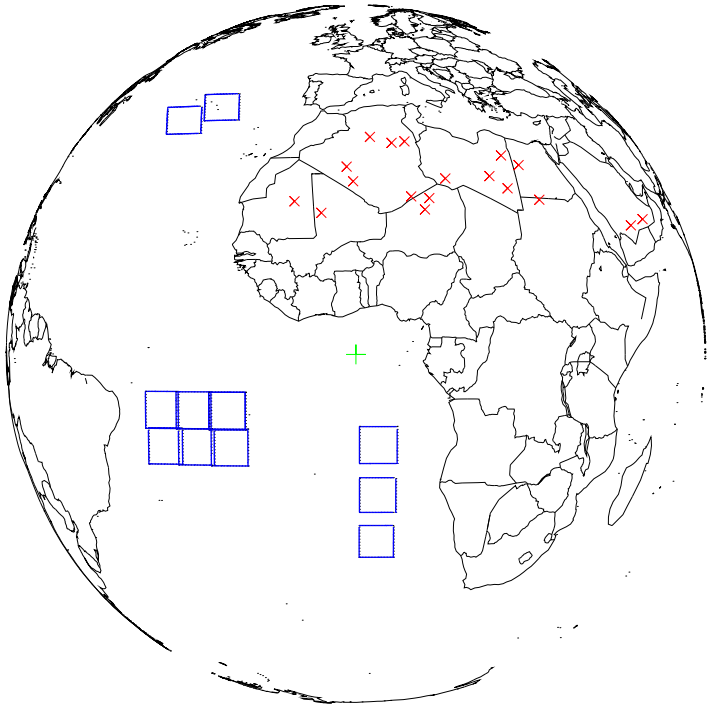

Figure 2: Location of the calibration targets for the 0° nominal sub-satellite position, shown with green "+" symbol. Desert target locations are indicated with the red × symbol and sea search areas with blue boxes.

3.2 Sea Surface

The aerosol optical thickness and surface wind speed are the two main state variables that govern the Top-Of-Atmosphere (TOA) radiance over sea surfaces in the SEVIRI solar bands. The ocean color, total column water vapor and ozone contribute also to the observed radiances, but only to a lesser extend. Hence, clear ocean areas used for the calibration have been chosen far from any continents, where the tropospherical aerosol and ocean pigment concentrations are expected to be minimum (Fig. 2). Simulations are performed with 6S code (Vermote et al. 1997), assuming a US62 vertical profile and oceanic aerosol type all year long. A climate data of set aerosol optical thicknesses corresponding to very clear days are derived from AErosol RObotic NETwork (AERONET) observations. Typical values range between 0.03 and 0.07. The surface wind speed and total column water vapor are taken from the European Centre for Medium-Range Weather Forecasts (ECMWF) analyzed data. A monthly mean ozone climate data set has been built from several years of TOMS observations, with a typical standard deviation of about 15%. The ocean color is determined for a fixed pigment concentration of 0.2 mgm^{-3}.

3.3 Bright Desert

A series of radiometrically stable and bright targets, located in the Saharan and Saudi Arabian deserts (see Fig. 2) have already been identified by Cosnefroy et al. (1996) and their stability confirmed by Capderou (1998). These arid targets are large uniform areas, essentially consisting of sand dunes, gravel and rocks. The surface bidirectional reflectance is represented with a simple bare soil model (Pinty et al. 1989), coupled with 6S radiative transfer code. This bare soil BRF model depends on three state variables, namely, the single scattering albedo, the asymmetry of the phase function and finally a porosity parameter. The value of these parameters over each site have been derived from POLDER observations (Bicheron and Leroy 2000). The retrieved model parameters have been spectrally interpolated to the SEVIRI bands, forcing the albedo to match typical bright

sand spectrums. Regarding the atmospheric properties, the principal state variables controlling TOA radiances over bright surfaces in the 0.4μm – 1.6μm spectral range are the total column water vapor, the total column ozone and the aerosol optical thickness. A US62 vertical atmospherical profile and desert dust aerosol type (Shettle and Fenn 1979) are assumed all year long. Aerosols have a limited impact on TOA radiance over bright surfaces, except in case of severe dust events. An aerosol optical thickness climate data set is derived from TOMS absorbing Aerosol Index and AERONET observations.

Table 2: Selected spectral bands for each instrument.

BAND		MERIS	ATSR-2	SeaWiFS	VGT
BLUE	0.4	442	–	443	B0
GREEN	0.5	560	550	555	–
RED	0.6	665	660	670	B2
NIR	0.8	865	870	865	B3
SWIR	1.6	–	–	–	MIR

3.4 Simulated radiance accuracy estimation

The accuracy and precision of these simulations, *i.e.*, the reference against which SEVIRI is calibrated, have been evaluated comparing simulations with calibrated observations acquired by spaceborne instruments (Govaerts and Clerici 2003). To this end, ERS2/ATSR-2, SeaStar/SeaWiFS, VEGETATION and Envisat/MERIS data have been collected over the desert targets simulated accounting for the actual observation conditions and spectral response of each instrument (Table 2). This analysis shows that the monthly mean relative bias between simulation and observation averaged over all targets remains low, but exhibits a small seasonal trend (Fig. 3). These results indicates that the reference can be used for the calibration of the SEVIRI solar channels with an expected accuracy of $\pm 5\%$ (Table 3) provided the calibration relies on the processing of a large number of observations. This error is lower than 3% in the SEVIRI VIS0.6 and VIS0.8 bands.

Table 3: Comparison between observations and simulations. r is the correlation coefficient. $\overline{\beta}_m$ is the mean relative bias in percent. $\sigma_{\overline{\beta}_m}$ is the standard error of $\overline{\beta}_m$.

BAND	BLUE (0.4)			GREEN (0.5)			RED (0.6)			NIR (0.8)			SWIR (1.6)		
SENSOR	r	$\overline{\overline{\beta}}_m$	$\sigma_{\overline{\overline{\beta}}_m}$	r	$\overline{\overline{\beta}}_m$	$\sigma_{\overline{\overline{\beta}}_m}$	r	$\overline{\overline{\beta}}_m$	$\sigma_{\overline{\overline{\beta}}_m}$	r	$\overline{\overline{\beta}}_m$	$\sigma_{\overline{\overline{\beta}}_m}$	r	$\overline{\overline{\beta}}_m$	$\sigma_{\overline{\overline{\beta}}_m}$
ATSR2	–	–	–	0.94	-2.0	5.10	0.97	1.4	3.57	0.98	2.2	3.17	–	–	–
SeaWiFS	0.95	1.4	4.57	0.91	-2.0	4.78	0.96	-1.1	2.97	0.96	2.7	2.97	–	–	–
VGT	0.96	0.5	4.81	–	–	–	0.98	4.9	2.66	0.98	5.2	2.89	0.92	-4.1	4.95
MERIS	0.96	8.3	5.00	0.93	0.9	4.55	0.98	2.8	1.85	0.98	6.1	1.75	–	–	–

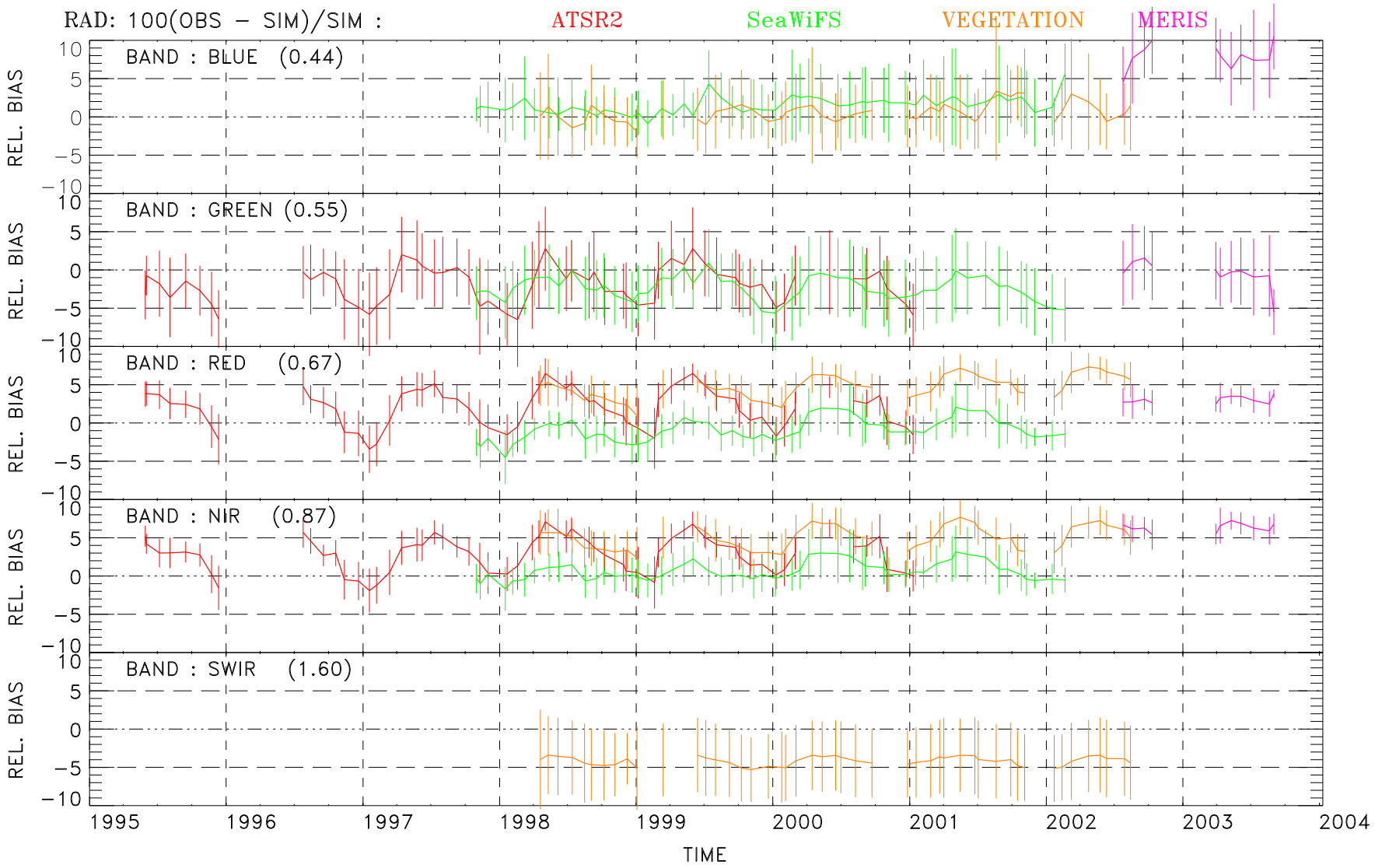

Figure 3: Monthly mean relative bias between observations and simulated radiances averaged over all desert targets in the blue, green, red, NIR and SWIR spectral regions. The standard error is shown with the vertical bars. The sensors are given the following color codes: ATSR-2 is in red, SeaWiFS in green, SPOT-4/VEGETATION in orange and MERIS in purple.

4 OPERATIONAL CALIBRATION METHOD

4.1 Overview

As seen in the previous section, the estimation of the calibration coefficient is affected by calibration reference uncertainties and the instrument characteristic errors. It is therefore necessary to estimate the corresponding impact on the calibration coefficient accuracy and, if possible, to minimize this error. The proposed calibration algorithm is thus designed to minimize the error propagation while deriving a calibration coefficient and to verify the consistency of this estimation. Calibration relying on the processing of a large amount of data should permit to reduce the errors, provided that these errors are independent and random, *i.e.*, not systematic. An error reduction methods has thus been developed and relies on a twofold strategy. Firstly, a target identification process aims at finding cases where the target parameter error is minimum. For instance, calibration over sea target will not take place when surface wind speed exceeds 7ms^{-1}, *i.e.*, when foam starts to appear at the sea surface. To increase the probability of finding such ideal situations, the calibration relies on the acquisition of data during a given processing period, of typically 5 to 10 days. Secondly, an error reduction based on temporal and spatial averaging of the results is applied to detect inconsistent results, if any, and to reduce the effects due to random errors. It is therefore necessary to discriminate systematic from random errors. Atmospheric properties are likely to change from day to day so that it is reasonable to assume that atmospheric parameter errors are not temporally correlated. Conversely, since desert target properties are very stable, any uncertainty in the characterization of these properties will be responsible for systematic errors in time. All errors are estimated for a given confidence level set to 95%.

4.2 Target Identification

For each analyzed image during a processing period, an identification process takes place to select potential targets whose actual properties and observation/illumination angles correspond to cases where calculated radiance error is minimum. Over desert targets, cloud and sand storm cases are identified analyzing daily variation of the observed count values. Clear sky pixel detection is performed fitting a second order polynomial to the daily cycle of observations. Any deviation from this polynomial is interpreted as a cloud contamination, cloud shadow or sand storm. Observations of that day are disregarded when the remaining number of clear sky slots is too low after this daily filtering. Sea targets are defined by large search areas in which cloud and aerosol free potential pixels are identified, looking at uniform and very low digital count values outside the sun-glint regions. This procedure is used to ensure a very low aerosol optical thickness.

When a target is successfully identified within an image acquired at time t, the $N_c \times N_l$ pixels centered on the target location are extracted from the corresponding image. The average value, minimum, maximum and error of the observed pixel count values over that site are next evaluated. The associated radiometric error is estimated at 95% confidence level accounting for both the instrument noise and any deviation from the target uniformity. Since targets are very uniform areas, the difference between the maximum and minimum count value within the target are expected to be very small. An observation is rejected when it is not the case.

4.3 Calibration

4.3.1 Calibration of individual observation

For all successfully identified targets, TOA radiances are calculated with the 6S code (Vermote et al. 1997) accounting for the illumination and viewing angles at the acquisition time and the surface and atmospheric properties. Simulated radiance errors are due to individual state variable error and the Radiative Transfer Model (RTM) intrinsic error, *i.e.*, imprecision of the numerical procedure not related to errors in the model

input parameters (Koepke 1982). Finally, the effective radiance is affected both by the uncertainty on the sensor spectral response characterization.

The time series composed of pairs of observed count / simulated radiance are accumulated individually for each target during the period. A calibration coefficient is estimated for each pair of the time series. The corresponding error is expressed as the quadratic sum of the relative radiance *i.e.*, surface and atmospheric parameterization error, RTM intrinsic error, SSR error and radiometric errors.

4.3.2 Temporal averaging

As the desert surface characteristics are supposed stable in time, only the instrument radiometric noise and atmospheric parameter uncertainty are responsible for temporal random errors. Calibration coefficients derived over each target are thus temporally averaged to reduce random error effects due to atmospheric parameter error and radiometric noises. An additional test is performed to verify the consistency of the mean coefficients derived over each desert targets. Simulation reliability is controlled exploiting the anisotropy signature of the surface responsible for observed count variations (Govaerts et al. 1998). Calculated radiance daily variations are thus be compared with observations. When both simulation and observation are consistent, it should be possible to retrieve the offset value. This retrieved offset value is compared with the actual one, derived from deep space observations. When the surface BRF and/or the aerosol load are not correct, simulated radiance corresponding to high Sun Zenith Angles (SZAs) might exhibit systematic biases with respect to those calculated for low (SZAs). Such situation will be responsible for an erroneous retrieval of the offset.

4.3.3 Spatial averaging

All the coefficients temporally averaged over each target are now spatially averaged, assuming that the surface characterization errors are not correlated. Since spectral properties of desert targets are quite similar, these coefficients should normally be very close, even in case of large errors in the characterization of the sensor response. Hence, outliers, if any, are expected to result from modelling errors and are disregarded. The calibration coefficient error is estimated assuming that the surface errors are not correlated as previously discussed.

4.3.4 Final consistency check

A final test is performed to verify the consistency of the final calibration coefficient and its associated error. To this end, a calibration coefficient is derived over sea in a similar way to the exception of the daily cycle analysis which is not applied. Calibration coefficients derived over desert and sea targets should be similar if i) the radiometer respond linearly to the incoming radiance intensity, ii) the characterization of the SSR is correct and finally iii) the radiative transfer simulations are reliable. When these conditions are met, the difference between the calibration coefficients derived over each target type should be smaller than the corresponding error. Still, the coefficients derived over desert and sea targets might be very close but still be affected by a similar bias. An additional test is therefore applied to verify the consistency of the results, based on a similar reasoning as in Section (4.3.2) to retrieve the space count. This test is performed accounting for all the observations over both sea and desert that have successfully passed all the previous consistency checks.

5 RESULTS

A 5 day period running from 4 to 8 August 2003 has been processed with the SSCC algorithm as part of the MSG calibration/validation commissioning activities. SEVIRI level 1.5 images were generated by the IMage

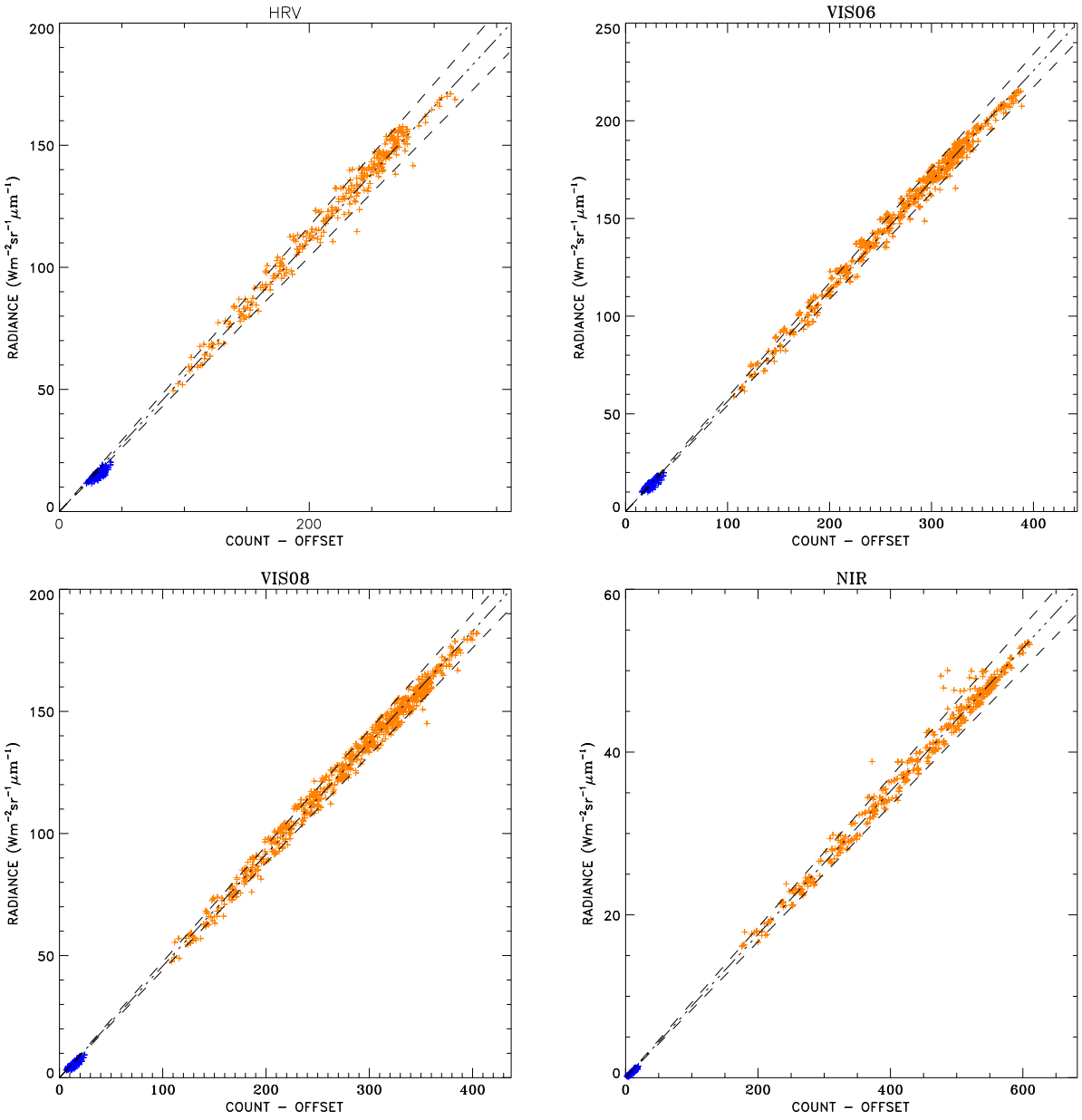

Figure 4: Scatter plot of the observed SEVIRI count values over the desert (orange + symbol) and sea (blue + symbol) calibration targets. Mean calibration slope in each band is shown with the dash-dotted line. The corresponding uncertainty is shown with the dashed lines. Offset value is equal to 51 Digital Count values for all solar channels.

Processing Facility (IMPF) of the MSG ground segment. The scatter plots of the observed SEVIRI count values *versus* the simulated radiances over desert and sea calibration target are shown on Fig. (4). As can be seen, the SEVIRI solar channels respond linearly with intensity. Results are summarized on Table (4). Calibration coefficients derived with SSCC are in good agreement with pre-launch values. The estimated error ranges from 4 to 6% according to the SEVIRI channel. These errors are slightly higher than the RTM accuracy estimation presented in Section (3.4). They appear thus realistic, in particular in the light of the retrieved offset values estimated in the final consistency check described in Section (4.3.4). These retrieved offset values are very close to the actual ones increasing thereby the confidence in the calibration results.

Table 4: SEVIRI calibration results for the processing period 4 – 8 August 2003. Calibration coefficients are given in $\mathrm{Wm^{-2}sr^{-1}}\mu\mathrm{m^{-1}}$/COUNT.

BAND	SSCC Cal. Coef.	Pre-launch Cal. Coef.	Offset	Retrieved Off.
HRV	$0.553 \pm 6\%$	$0.498 \pm 10\%$	51	54
VIS0.6	$0.564 \pm 4\%$	$0.578 \pm 10\%$	51	51
VIS0.8	$0.467 \pm 4\%$	$0.397 \pm 10\%$	51	52
NIS1.6	$0.088 \pm 5\%$	$0.081 \pm 10\%$	51	53

6 CONCLUSION

The calibration reference used for the operational vicarious calibration of the SEVIRI solar channels consists of simulated TOA radiances over bright desert targets, using a data set of surface and atmospheric properties. The accuracy and precision evaluation of this reference relies on a comparison between calibrated spaceborne data and their simulation. These comparisons reveal that the relative bias between simulations and calibrated observations does not exceed 3% in the VIS0.6 and VIS0.8 bands with respect to ATSR-2 and SeaWiFS, when a large number of observation are averaged over all targets. These comparisons also reveal the very similar radiometric behavior of the ATSR-2 and SeaWiFS radiometers.

The SSCC algorithm has already been successfully applied for the calibration of the SEVIRI solar channels. Although calibration error estimation is still on-going, preliminary commissioning results are encouraging. After the MSG commissioning period, the SSCC algorithm will be routinely applied to calibrate the solar channels and to monitor the long-term sensor drift.

References

Bicheron, P. and M. Leroy (2000). BRDF signatures of major biomes observed from space. *JGR 105*, 26,669–26,682.

Capderou, M. (1998). Study of the stability of the ScaRaB shortwave channel. Application: determination of uniform desert zone. *International Journal of Remote Sensing 19*, 3641–3669.

Cosnefroy, H., M. Leroy, and X. Briottet (1996). Selection and characterization of Saharan and Arabian desert sites for the calibration of optical satellite sensors. *Remote Sensing Environment 58*, 101–114.

Govaerts, Y. M. and M. Clerici (2003). Evaluation of Radiative Transfer Simulations over Bright Desert Calibration Sites. *IEEE Transactions on Geoscience and remote sensing in print*.

Govaerts, Y. M., B. Pinty, M. M. Verstraete, and J. Schmetz (1998). Exploitation of angular signatures to calibrate geostationary satellite solar channels. In IEEE (Ed.), *IGARSS'98*, Seattle, USA, pp. 327–329.

Koepke, P. (1982). Vicarious satellite calibration in the solar spectral range by means of calculated radiances and its application to Meteosat. *Applied Optics 21*, 2845–2854.

Pinty, B., M. M. Verstraete, and R. Dickinson (1989). A physical model for predicting bidirectional reflectances over bare soil. *Remote Sensing of Environment 27*, 273–288.

Schmetz, J., P. Pili, S. Tjemkes, D. Just, J. Kerkmann, S. Rota, and A. Ratier (2002). An introduction to Meteosat Second Generation. *Bulletin of the American Meteorological Society 83*, 977–992.

Shettle, E. P. and R. W. Fenn (1979). Models for the aerosols of the lower atmosphere and the effects of humidity variations on their optical properties. Technical Report AFGL-TR-79-0214, U.S. Air Force Geophysics Laboratory, U.S. Air Force Geophysics Laboratory.

Vermote, E. F., D. Tanré, J. L. Deuzé, M. Herman, and J. J. Morcrette (1997). Second simulation of the satellite signal in the solar spectrum, 6S: An overview. *IEEE Transactions on Geoscience and Remote Sensing 35*, 675–686.